

Research on the Strain Prediction Method of High-Temperature Pressure Vessel Based on Finite Element and Deep Learning

Wenjie Li^a, Yufeng Tang^{*}, Siwei Zhang, Rui Cao

Sichuan University of Science and Engineering, School of Mechanical Engineering, Yibin 644002, China

^a573043571@qq.com; ^{*}Corresponding Author: 386426034@qq.com

ABSTRACT

The stress and strain of metals under high-temperature operation have significant implications for the optimal design and safety assessment of high-temperature pressure vessels. However, it is challenging to efficiently evaluate the stress and strain in critical parts of high-temperature pressure vessels. To address these issues, a method combining deep learning and finite element analysis is proposed to predict the total strain of high-temperature pressure vessels. Firstly, finite element simulations are conducted under multiple working conditions and sizes to provide data support for deep learning prediction. Secondly, the WOA algorithm is used to optimize the number of hidden layer neurons and learning rate for LSTM, and the optimized hyperparameters are then assigned to the LSTM network to construct a prediction model that matches the data features more effectively. Finally, the data obtained from the finite element simulations are fed into the prediction model, and the results show that the prediction accuracy reaches 98.6%, demonstrating good predictive performance. This achievement can provide efficient data support for the optimal design and safety assessment of high-temperature pressure vessels.

KEYWORDS

Finite Element; High-Temperature Pressure Vessel; Deep Learning

1. INTRODUCTION

As pressure equipment, pressure vessel is widely used in national defense, material transportation, aerospace engineering, nuclear power and other fields. At the same time, it is a special equipment with high explosion risk[1]. Especially in the nuclear power, petrochemical, nuclear industry and other fields, many equipment service in high temperature and pressure environment for a long time[2]Lower, such as the thermal end parts of a nuclear reactor[3], Expansion joints for catalytic cracking pipes, boiler steam pipes, chemical containers and thermal instruments, and constrained expansion joints[4-5]. These equipment operate for a long time under high temperature and high pressure conditions, resulting in the failure of materials different from normal temperature equipment, that is, creep fracture and failure. Therefore, fatigue creep is the important factor of high temperature life prediction.

Specification case ASME Code Case 2605 [6] provides a 2.25Cr1MoV. Qin Shujing[7]The principle and application scope of this method are introduced. Wan Li equality[8]The relevant factors of this design method were analyzed. There are many factors that affect the life of metal materials at high temperatures and variable load environments. For example, according to the ASME Nuclear Power Code and Standard ASME BPVC Division 5 High Temperature Reactors (2015) on high temperature strain, deformation and fatigue limits[9], The factors that affect the fatigue creep life of the component

include the maximum temperature of the node on the key path, the primary stress limit of the node, the secondary stress limit, the high temperature duration, the secondary stress range, and the key factors of the primary and secondary stress amplitude. Therefore, the real-time stress and strain monitoring of each critical site is very difficult. In addition, due to the design and operation of pressure vessels, the stress strain prediction even by methods such as finite element. To address the above problems, this paper proposes a combination of finite element steady-state thermal simulation and deep learning[10]Methods for the safety assessment of high-temperature pressure vessels[11]. First, steady-state thermal and static simulation of pressure vessels. Set them at different temperatures, different sizes, and different pressures. Secondly, combined with deep learning technology, the strain of key parts of a high temperature pressure vessel generator is predicted with different temperatures, sizes and pressures as inputs. Through this study, we can deeply understand the thermodynamic performance of key parts in high-temperature pressure vessels, and predict their key characteristic parameters in different working conditions. It helps to optimize the design and improve the process to improve the safety and reliability of the pressure vessels.

2. RELEVANT PRINCIPLES

2.1. LSTM model

LSTM solves the problem of gradient explosion or gradient disappearance in traditional RNN during training, which is caused by the increase of RNN with training time and the number of network layers. LSTM not only adds a new hidden cell state in the structure, but also designs various "gate" structures to increase or reduce the information to the cell state, which can specifically control the input data through the "gate". This kind of data transmission mode makes the weight of the self-loop no longer fixed, and can have a memory function for a long time[12]. Therefore, LSTM has a strong advantage in the prediction and classification of the time series.

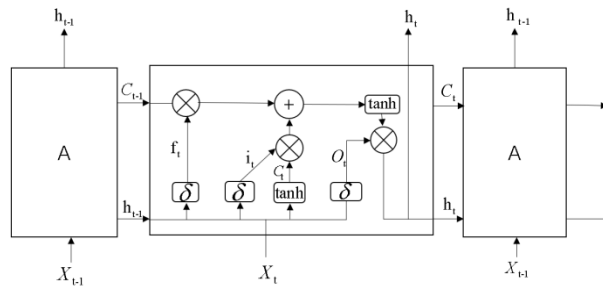


Figure 1. Structural diagram of the LSTM

X_t, C_{t-1} The structure of a single LSTM unit is described above as shown in Figure 1. At each time step, the input and previous cell states are processed through three gates: forgetting gate (Forget Gate), input gate (Input Gate), and output gate (Output Gate). The forgetting gate determines how much information to discard from the cell state, the input gate determines how much new information to add to the cell state, and the output gate determines how much information to output from the current cell state. Finally, the calculated cell state and output will serve as input for the next time step. The principle of the LSTM is as follows: C_t, h_t

Input gate (Input Gate): the calculation that determines whether to incorporate the current input information into the internal memory state.

$$f_t = \sigma[\mathbf{W}_f(h_{t-1}, X_t) + b_f] \quad (1)$$

$$i_t = \sigma[\mathbf{W}_i(h_{t-1}, X_t) + b_i] \quad (2)$$

$$\tilde{C}_t = \tanh \sigma[\mathbf{W}_c(h_{t-1}, X_t) + b_c] \quad (3)$$

$$C_t = f_t C_{t-1} + i_t \tilde{C}_t \quad (4)$$

$$o_t = \sigma[\mathbf{W}_0(h_{t-1}, X_t) + b_0] \quad (5)$$

$$h_t = o_t \cdot \tanh(C_t) \quad (6)$$

$\mathbf{W}_i, \mathbf{W}_f, \mathbf{W}_0, \mathbf{W}_c, b_i, b_f, b_0, b_c, h_{t-1}, X_t$ Where, is the weight matrix, is the bias vector, representing the combination of the hidden layer state and the current input at the previous moment. \tanh For the hyperbolic tangent activation function.

Forget gate (Forget Gate): decide whether to forget part of the previous memory state. How much old information is forgotten by a sigmoid function. Cell state (Cell State) Update: Update the cell state based on the results of the input gate and the forgetting gate. Output gate (Output Gate): determines how much information to output from the current cell state. How much information is output by a sigmoid function. Hidden layer state (Hidden State) Update: using the output gate and the updated cell state. The hidden layer state is the final output of the LSTM model.

2.2. Whale optimization algorithm

The whale optimization algorithm was proposed by the Australian Mirjalili in 2016[13]. The whale optimization algorithm is an optimization algorithm to simulate the humpback whale hunting strategy, which has the advantages of simple algorithm, strong search ability and fast convergence speed. The algorithm consists of three stages: surround the prey, bubble net attack and search for prey.

During the enclosure phase, the humpback whale gradually surrounds the prey by constantly adjusting its position. Individuals update their position based on the current search agent location closest to the prey, while others approach the optimal individual location. Where is the distance between the current individual position and the optimal individual position, $\mathbf{X}(t)$ represents the position vector of the current individual, and the parameter vector, updated by the random number and the number of iterations. $\mathbf{D}, \mathbf{A}, \mathbf{C}$

$$\mathbf{D} = |\mathbf{CX}^*(t) - \mathbf{X}(t)| \quad (7)$$

$$\mathbf{X}(t+1) = \mathbf{X}^*(t) - \mathbf{AD} \quad (8)$$

In formula (7) (8), \mathbf{D} is the distance between the current individual position and the optimal individual position; it is the position vector of the optimal individual; $\mathbf{X}^*(t)$

$\mathbf{X}(t+1)$ Is the position vector of the current individual; t is the current number of iterations; and are both parameter vectors, and their expressions are respectively: \mathbf{A}, \mathbf{C}

$$A = a \cdot (2r_1 - 1) \quad (9)$$

$$C = 2r_2 \quad (10)$$

$r_1, r_2 \sim$ In equation (9) (10), the random number between 01; a decreases linearly from 2 to 0 with the number of iterations, as follows:

$$a = 2 \cdot (1 - t / t_{\max_iter}) \quad (11)$$

During the bubble net attack phase, the humpback whale moves forward in a spiral motion and gradually shrinks the enclosure. Depending on the selection probability, the individual has a certain probability of choosing to contract around or spiral forward. In this model of probabilistic selection, p is the random number, l is constant, r is the distance between the current individual and the optimal individual, b is constant, generally take 0.5. As the number of iterations increases, individuals tend to

linearly decreasing a values, fluctuating between [-a, a]. When less than 1, individuals will attack their prey. This mathematical model of synchronous selection can be expressed as follows: P_i A A

$$\mathbf{X}(t+1) = \begin{cases} \mathbf{X}^*(t) - \mathbf{AD}, & p < P_i \\ \mathbf{De}^{bl} \cos(2\pi l) + \mathbf{X}^*(t), & p \geq P_i \end{cases} \quad (12)$$

Where p is the random number between 0 and 1; it is (1,1); l

$\mathbf{D}' = |\mathbf{X}(t) - \mathbf{X}^*(t)|$ For the current distance between each individual and the optimal individual.

During the prey search phase, the individual search mechanism is determined according to the size of A. When A is less than 1, individuals will search locally against the optimal individual location. When A is greater than 1, individuals move away from the current optimal individual position for a global search based on randomly selected locations.

The mathematical model for performing the global search at A A greater than 1 is as follows:

$$\mathbf{D} = |\mathbf{CX}_{\text{rand}}(t) - \mathbf{X}(t)| \quad (13)$$

$$\mathbf{X}(t+1) = \mathbf{X}_{\text{rand}}(t) - \mathbf{AD} \quad (14)$$

2.3. WOA-LSTM algorithm

WOA optimization of the LSTM algorithm: the WOA algorithm is applied to the optimization process of the LSTM model[14]centre. The specific steps are described as follows:

- a. Initialization: Initialize the parameters of the LSTM model, such as weights and bias, using the WOA algorithm.
- b. Training phase: train the LSTM model with the training data to calculate the loss function. Here, parameter updates can be performed using conventional back-propagation algorithms or other optimization algorithms.
- c. WOA operation: In each iteration, the parameters of the LSTM model are adjusted and optimized according to the current number of iterations and the update equation of the WOA algorithm. The WOA algorithm will guide the update of the parameters based on the change of the individual position and the optimal individual position.
- d. Termination condition: Set the appropriate stop condition, such as reaching the maximum number of iterations or loss function convergence.

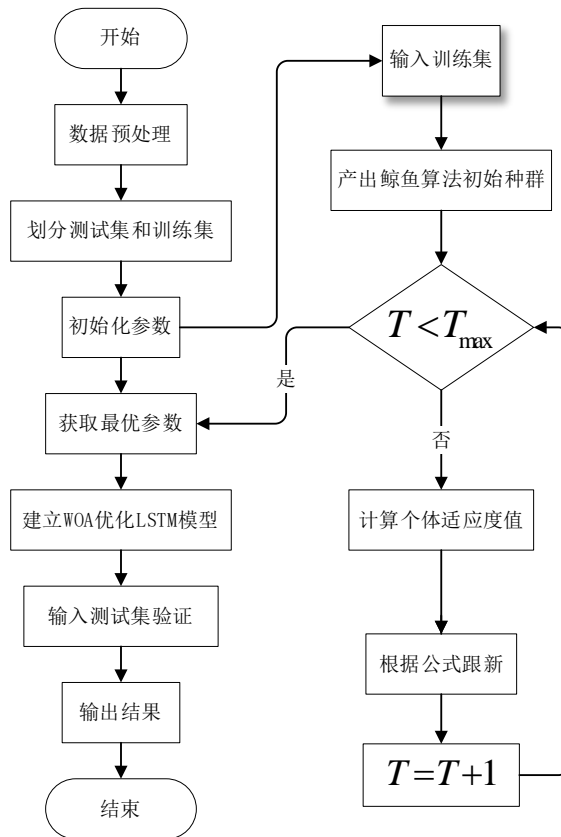


Figure 2 Flow of WOA-L STM model construction

Through the above steps, WOA optimizes the LSTM algorithm[15]Be able to combine the global search features of the WOA algorithm and the memory ability of the LSTM network during training to improve the performance and effect of the LSTM model on sequence data. This approach enables better exploration of the parameter space and finding better parameter settings, thereby improving the modeling and predictive capabilities of the sequence data.

3. HIGH-TEMPERATURE SIMULATION OF THE PRESSURE VESSEL

In the modeling process, the key parts of the generator of a high temperature pressure vessel is used for the FE analysis, as shown in Figure 3, the generator is at different temperatures (300°C -900°C), different thicknesses (12CM-15CM), the key parts under different pressures (2MPa-4MPa), and the maximum deformation of the key position is calculated by multiple numerical simulation experiments with a total of 160 sets of experimental data. Fig. 3 is the setting of steady-state thermal simulation and statics simulation. Fig. 4 is the strain cloud diagram, and Figure 5 is the path diagram at the maximum strain.

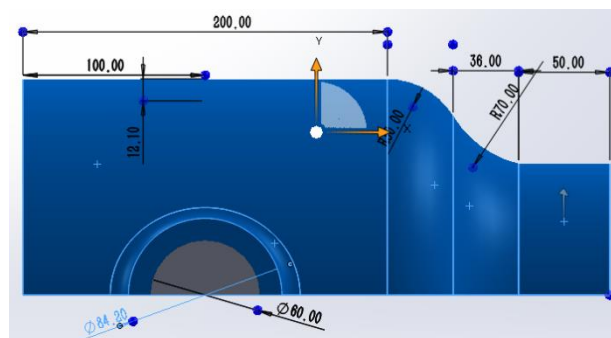


Figure 3 Size diagram

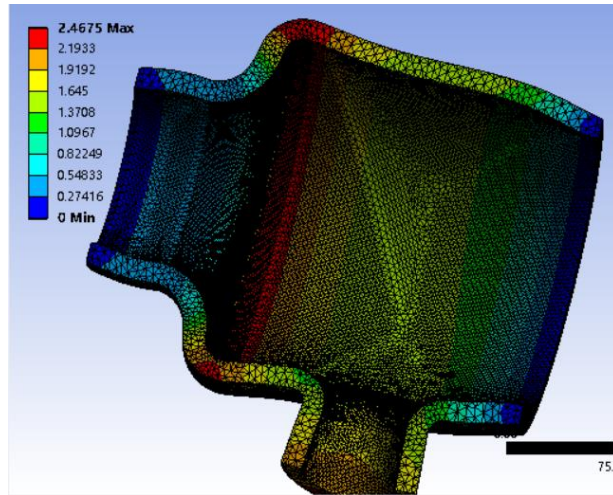


Figure 4 Strain cloud diagram

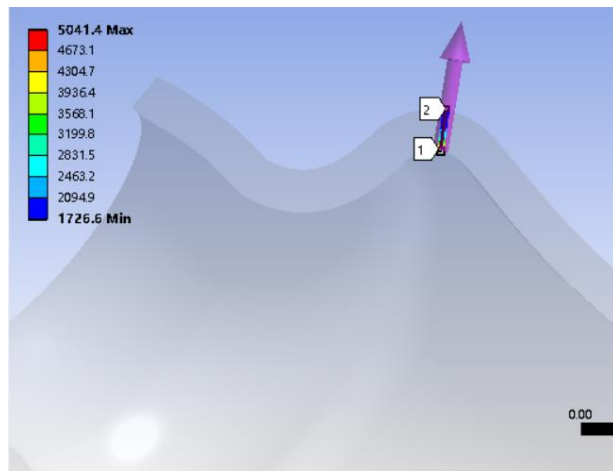


Figure 5 the path at maximum strain

Table 1. Performance parameters of the materials

density (kg/m ³)	Poisso n ratio	Elastic modulu s (GPa)	Thermal conductivity coefficient W / (mC)	Specific heat capacity J / (kg C	Thermal expansion coefficient (10- 6/°C)	Alable stress (MPa)
7895	0.31	200	60.5	501	14.1	151

In Table 1, the specific heat capacity =TC / (TD density)

After the simulation of high temperature pressure vessel data, the average time of each set of data from the modification of the structural model, dividing the grid, setting the parameters to the final simulation results is 10 minutes, while the simulation of a large amount of data requires a lot of time.

4. THE MAXIMUM STRAIN PREDICTION OF HIGH-TEMPERATURE PRESSURE VESSELS BASED ON DEEP LEARNING

4.1. Setting of the experimental parameters

To verify the performance of the WOA-LSTM network, the model structure includes the input layer, two LSTM layers and the output layer, the loss function uses the mean square error, and the hidden layer parameters of the LSTM network use the adaptive moment estimation method. Set the maximum number of training rounds is 250,160 sets of data in order, divided into training set 120

groups, 40 test set, the hidden layer node L1, L2, LSTM model, the learning rate Lr by the whale algorithm, in order to prevent the search space of the efficiency of the WOA, the initial range is set to [1,100], [1,100] and [0.001,0.01], and then iterative optimization, to find the optimal hyperparameters. At the same time, the population number of the whale algorithm is set to 40, the maximum number of iterations is 30, the input is the pressure, temperature, size, and the output is the maximum strain.

4.2. Analysis of the results

In order to comprehensively analyze the effectiveness and accuracy of the prediction model, the following four indicators are selected to evaluate it [16], The average absolute error (mean absolute error, MAE), also known as the absolute error, is applicable to the difference between the predicted value and the actual observed value is more obvious. Because the average absolute error can avoid the problem of error canceling each other, and can accurately reflect the error between the predicted value and the true value. The root mean square error (root mean square error, RMSE) is the arithmetic square root of the mean square error and the square root of the sum of the deviation of the prediction from the true value to the number of observations n. The average absolute percentage error (mean absolute percentage error, MAPE) means that the error of each point is normalized, which partly reduces the effect of individual outliers on the absolute error. The smaller the MAPE is, the better the model is. The average absolute percentage error (mean absolute percentage error, MAPE) means that the error of each point is normalized, partly reducing the effect of individual outliers on the absolute error. When the MAPE is smaller, the smaller is the representative model. goodness of fit R² The ability of the model to explain the variability of the dependent variable was measured. It represents the proportion of the correlation between the predicted model and the actual observations, ranging between 0 and 1. R² The closer to 1, the better the model fits to the data.

$$MAE = \frac{1}{n} \sum_{i=1}^n |y_i - \hat{y}_i| \quad (15)$$

$$RMSE = \sqrt{\frac{1}{n} \sum_{i=1}^n (y_i - \hat{y}_i)^2} \quad (16)$$

$$RMSE = \sqrt{\frac{1}{n} \sum_{i=1}^n (y_i - \hat{y}_i)^2} \quad (17)$$

$$R^2 = 1 - \frac{\sum_{i=1}^N (y_i - \hat{y}_i)^2}{\sum_{i=1}^N (y_i - \bar{y}_i)^2} \quad (18)$$

y_i \hat{y}_i \bar{y}_i (18) Where: N is the total number of samples, the predicted value of the first sample, the observed value of the first sample, and the average of the observed value of all samples. The evaluation index of each model can be obtained from the experimental data obtained in Section 3.1 from formula (15) to (18), as shown in Table 2.

Table 2 Results of the evaluation indicators of the WOA-LSTM model

prediction model	Training set error	Test set error
M AE	6.3561	6.5425
R MSE	7.7133	8.164
M APE	3.3779%	3.7087%
R2	0.98425	0.98669

It can be seen in the evaluation index diagram of the first two models of the training set error and test set error error is very small, illustrates the data division is reasonable, the results of the results of the average absolute error (MAPE) error of the test set is 3.708%, the MAPE of the test set 40 groups as shown in Figure 6, according to Table 1 and figure 7 root mean square error (RMSE) and goodness of fit of the test set (R2) Look, the effect is good, reaching 98.66%, and it is relatively stable after 27 iterations, as shown in Figure 8.

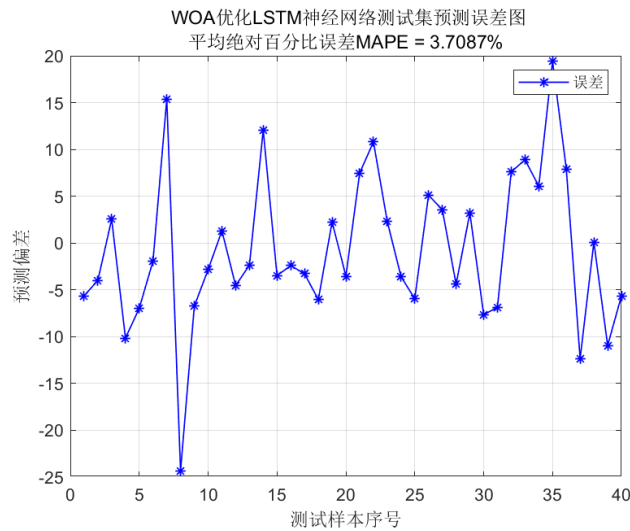


Figure 6 MAPE result plots for the test set and real values

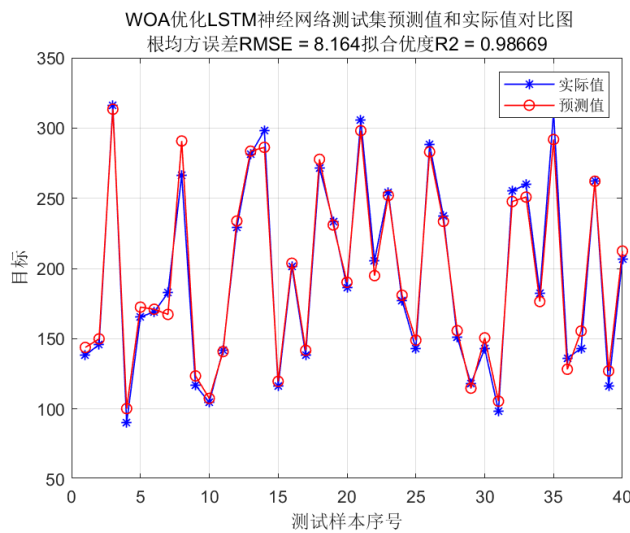


Figure 7 R M S E and R for the test set and actual values2Results of the figure

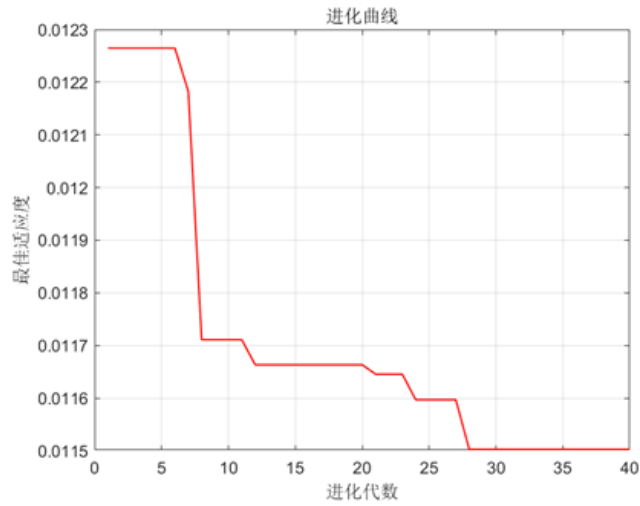


Figure 8 Fitness plot of WOA-LSTM

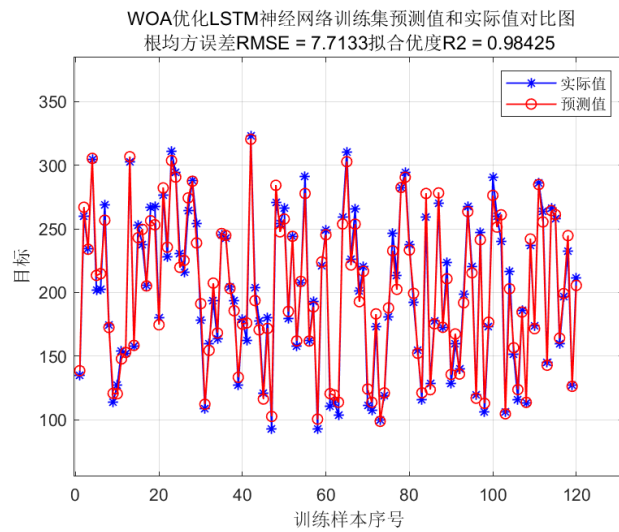


Figure 9 RMSE and R for the training set and actual values 2Results of the figure

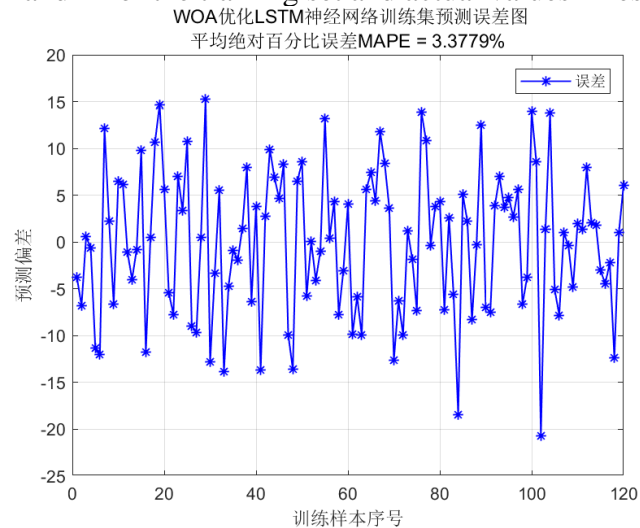


Figure 10 MAPE for the training set and actual values, and the results Fig

RMSE and R from the training set of Figure 9 and Figure 10. The effect of the training set is also good, reaching 98.425% and MAPE is 3.37%. The error comparison diagram of the WOA-LSTM network shows that MAE, RMSE, MAPE and R were used. By analyzing the error results, we can

intuitively see the prediction performance of the four algorithms. By setting, the number of populations is 40, the maximum number of iterations is 30, and the simulation takes about 8 minutes.

5. CONCLUSION

A strain prediction method of high temperature pressure vessel combined with finite element steady state thermal simulation and deep learning is proposed. The steady state thermal simulation of high temperature pressure vessel is firstly, and then the prediction model is constructed with WOA-LSTM neural network. By comparing the error data between predicted value and actual value, the following conclusions are drawn:

- (1) The WOA algorithm was used to optimize the structural parameters of the LSTM neural network, to solve the optimization problem of continuous weight and threshold, and then the prediction was successfully realized.
- (2) The proposed WOA-LSTM network model has a high accuracy of 98.6%.
- (3) The data obtained through the simulation of high temperature pressure vessel is output as a total deformation, which can play an important role in the safety estimation of high temperature pressure vessel.
- (4) By comparing the time used in the steady-state thermal simulation with the time used in the deep learning method, it shows that this method can greatly reduce the calculation workload and calculation time.

ACKNOWLEDGEMENTS

Science and Technology Support Project of Sichuan Provincial Science and Technology Department (2022NSFSC1154)

REFERENCE DOCUMENTATION

- [1] MAO Zhihui, Long Wei, Liu Huaguo, et al. Analysis of the extended life of pressure vessels with crack defects based on damage mechanics and safe attenuation path [J]. *Science, Technology and Engineering*, 2020,20 (27): 11105-11110
- [2] Chen Xuedong, Fan Zhichao, Cui Jun, Chen Yongdong, Zhang Xiaohu, Cheng Jingwei. Progress of high-performance manufacturing technology of pressure vessels in China [J]. *Pressure vessel*, 2021,38 (10): 1-15
- [3] Li Yongsheng, Li Jianguo. Application technology, design, manufacture and application of waveform expansion joint [M]. Beijing: Chemical Industry Press, 2000.
- [4] Yang Licai, Qiu Tian, Yang Zhihai, etc. Study on high temperature creep of lower pressure vessel head of Hualong 1 reactor [J]. *Nuclear Power Engineering*, 2022,43(S2):202-207.DOI:10.13832/j.jnpe.2022.S2.0202
- [5] Su Dongchuan, Zhang Ying, Du Juan, etc. Research on the constitutive model of 16 M ND 5 steel for domestic reactor pressure vessel [J]. *Nuclear Power Engineering*, 2022,43(01):232-237.DOI:10.13832/j.jnpe.2022.01.0232.
- [6] ASME Boiler and Pressure Vessel Code Case 2605-4[S].2021.
- [7] Qin Shu Jing. Evaluation method of creep intensity based on the Omega method [J]. *Chemical Equipment and Pipeline*, 2017, (Phase 5).
- [8] Wanli Ping, Li Yu. Design method of the 2.25 Cr-1Mo-V steel hydrogenation reactor considering the creep action [J]. *Pressure vessel*, 2021, (Phase 12): 62-69
- [9] Shen Jun, Chen Zhiwei, Liu Yinghua. Interpretation and discussion of the high temperature analysis method in ASME Specification Case 2843 [J]. *Pressure vessel*, 2018,35 (12): 47-55 + 68
- [10] Wu Neng and the same. Research on the structural optimization method of key components of pressure vessel based on intelligent algorithm [D]. Zhejiang University of Technology, 2019

- [11] Xuan Fuzhen, Tu Shandong, Wang Zhengdong and so on. Research progress in detection and safety assessment technology of used pressure vessels in high temperature environment (ii) —— assessment method [J]. Pressure vessel, 2002 (10): 1-5 + 12-20.
- [12] Yao Ning, Jin Xiuzhang, Li Yangfeng. NOX modeling of denitration system based on improved whale algorithm optimization of Bi-LSTM [J / OL]. Journal of North China Electric Power University (Natural Science Edition): 1-9 [2021-11-06].<http://kns.cnki.net/kcms/detail/13.1212.TM.20211015.2142.002.html>.
- [13] Yao Ning, Jin Xiuzhang, Li Yangfeng. NOX modeling of denitrification system by Bi-LSTM optimized with improved whale algorithm [J/OL]. Journal of North China Electric Power University: 1-9 [2021-11-06].<http://kns.cnki.net/kcms/detail/13.1212.TM.20211015.2142.002.html>
- [14] Mirjalili S, Lewis A The whale optimization algorithm [J]. Advances in Engineering Software, 2016, 95: 51-67
- [15] Liu Kun, Zhao Lulu, Wang Hui. Whale optimization algorithm based on elite opposition-based and crisscross optimization [J]. Journal of Chinese Computer Systems, 2020, 41(10): 2092-2097.
- [16] Hao Keqing, Lv Zhigang, Di Ruohai and so on. Prediction of residual life of lithium battery based on long-short memory neural network optimization by whale algorithm [J]. Science, Technology and Engineering, 2022, 22 (29): 12900-12908.
- [17] Huang Chenhong, Li Kunpeng, Zheng Zhen, et al. Short-term load prediction based on quadratic mixed mode decomposition and LSTM-MFO algorithm [J]. Electrical appliances and energy efficiency management Technology, 2022. (9): 66-73.